

# A bio-compatible pyridine-pyrazole hydrazide based compartmental receptor for Al<sup>3+</sup> sensing and its application in cell imaging

Bhriguram Das,<sup>a,b</sup> Malay Dolai,<sup>c</sup> Avijit Ghosh,<sup>d</sup> Anamika Dhara,<sup>e</sup> Ananya Das Mahapatra,<sup>f</sup> Debprasad Chattopadhyay,<sup>f,g</sup> Subhabrata Mabhai,<sup>h</sup> Atanu Jana,<sup>\*i</sup> Satyajit Dey,<sup>\*b</sup> and Ajay Misra<sup>\*a</sup>

<sup>a</sup>Department of Chemistry, Vidyasagar University, Midnapore-721102, West Bengal, India. E-mail: [ajay@mail.vidyasagar.ac.in](mailto:ajay@mail.vidyasagar.ac.in) ; [ajaymsr@yahoo.co.in](mailto:ajaymsr@yahoo.co.in) . Fax: +91 3222 275329

<sup>b</sup>Department of Chemistry, Tamralipta Mahavidyalaya, Purba Medinipur 721636, India. Email: [satyajitdeyoc@gmail.com](mailto:satyajitdeyoc@gmail.com)

<sup>c</sup>Department of Chemistry, Prabhat Kumar College, Contai, Purba Medinipur 721404, West Bengal, India.

<sup>d</sup>Center for Research in Nanoscience and Nanotechnology, Technology Campus, University of Calcutta, Salt Lake, Kolkata 700106, India

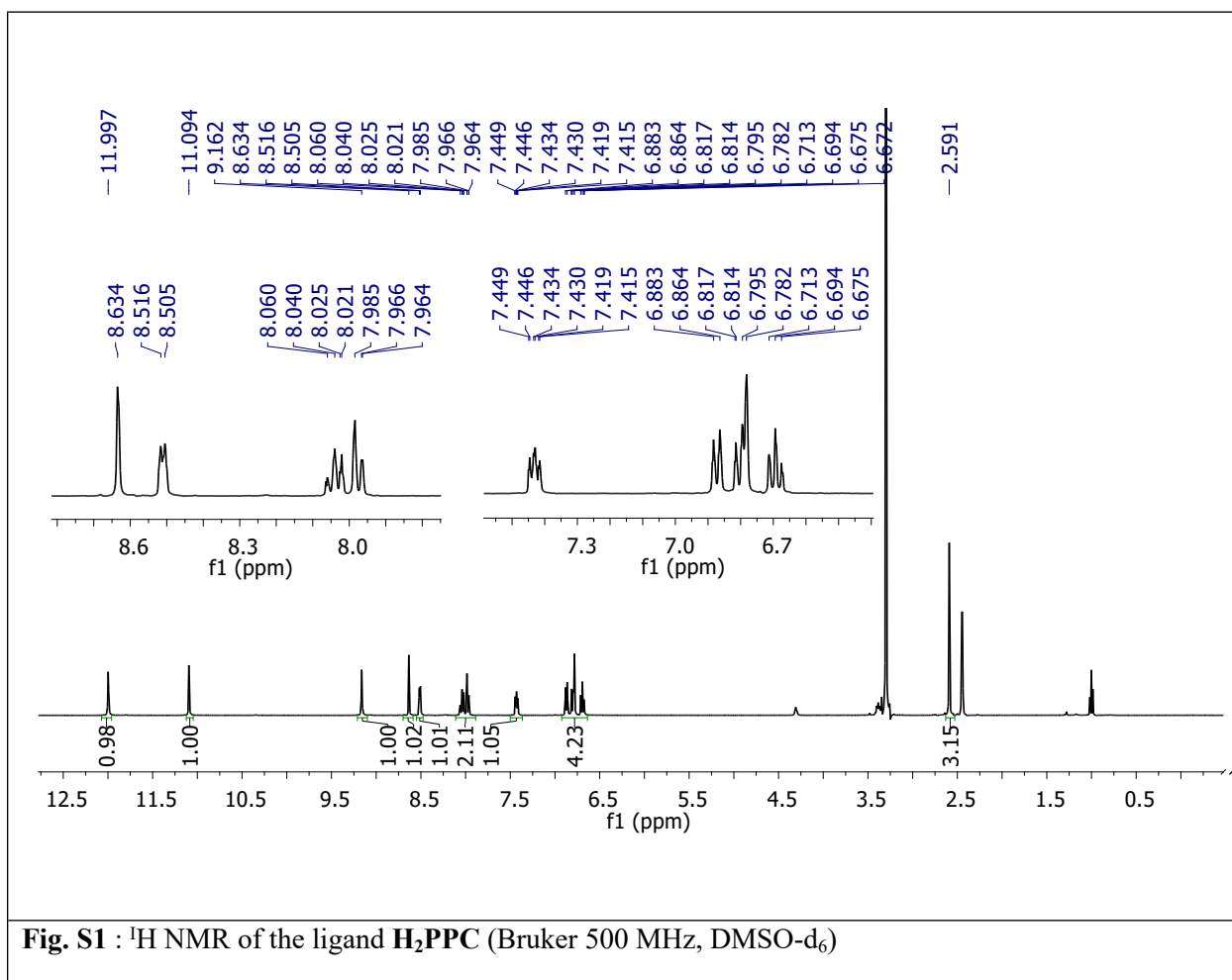
<sup>e</sup>Department of Chemistry, Hiralal Mazumdar Memorial College For Women, Dakshineswar, North 24 Parganas, Kolkata 700035, India

<sup>f</sup>ICMR-Virus Unit, ID & BG Hospital Campus, 57 Dr Suresh C Banerjee Road, Beliaghata, Kolkata 700010, India

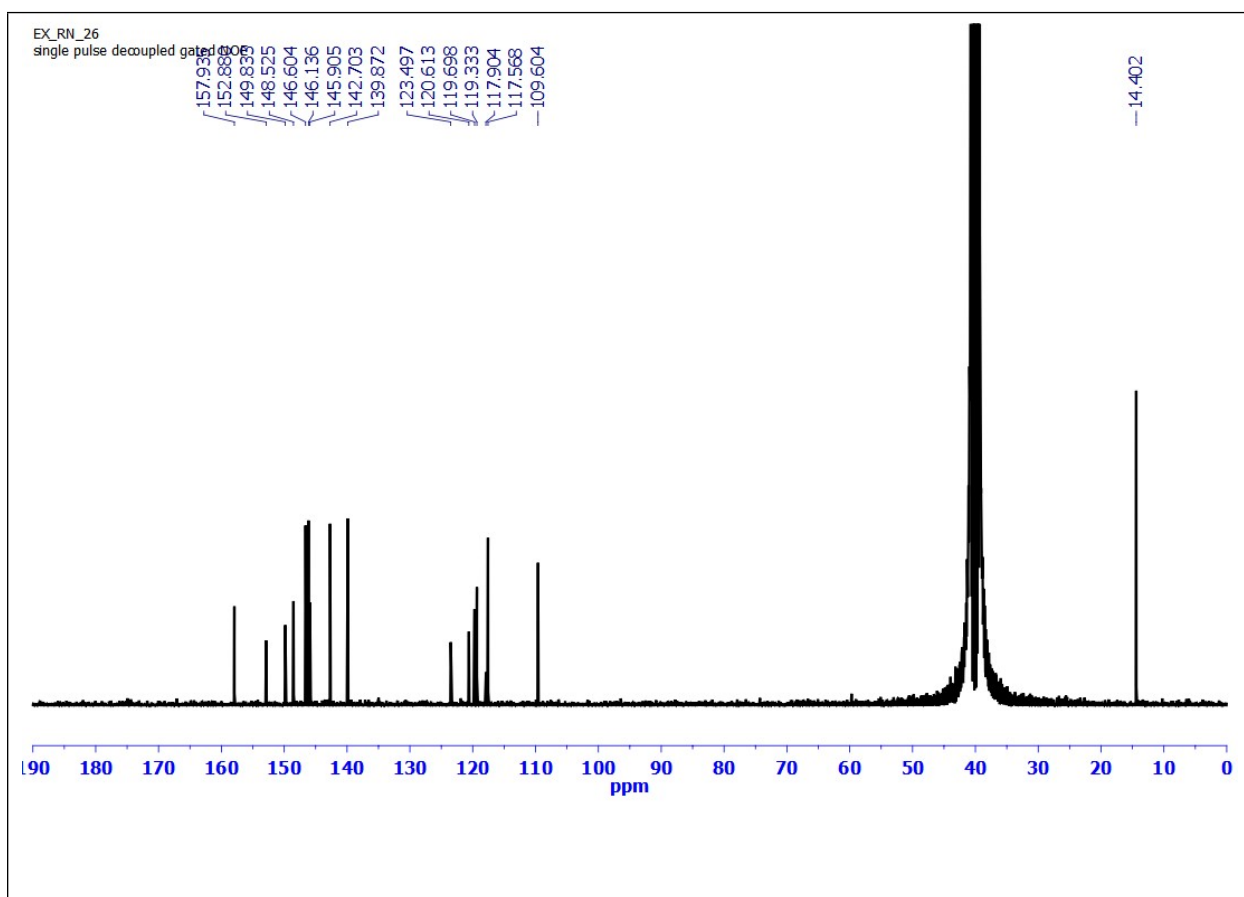
<sup>g</sup>ICMR-National Institute of Traditional Medicine, Nehru Nagar, Belagavi 59001 Karnataka, India

<sup>h</sup>Department of Chemistry, Mahishadal Raj College, Purba Medinipur, 721628, India

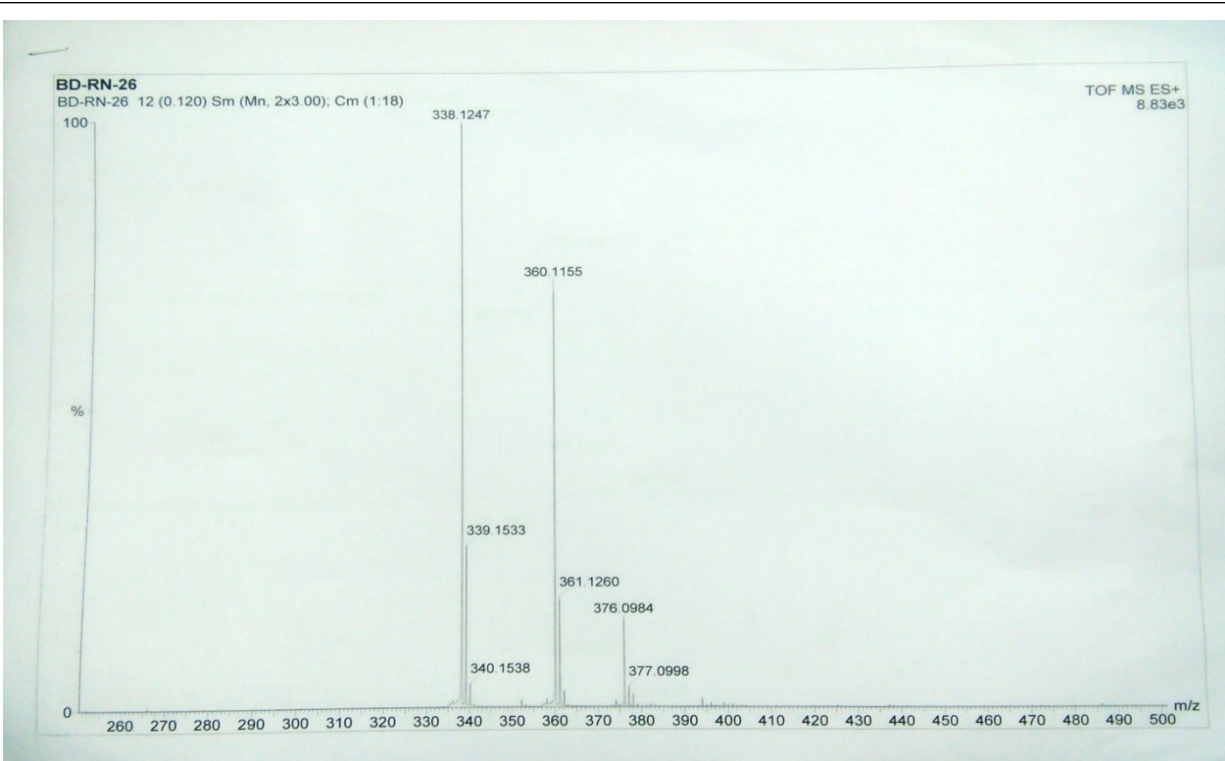
<sup>i</sup>Division of Physics and Semiconductor Science, Dongguk University, Seoul, 04620, South Korea. Email: [atanujanaic@gmail.com](mailto:atanujanaic@gmail.com)



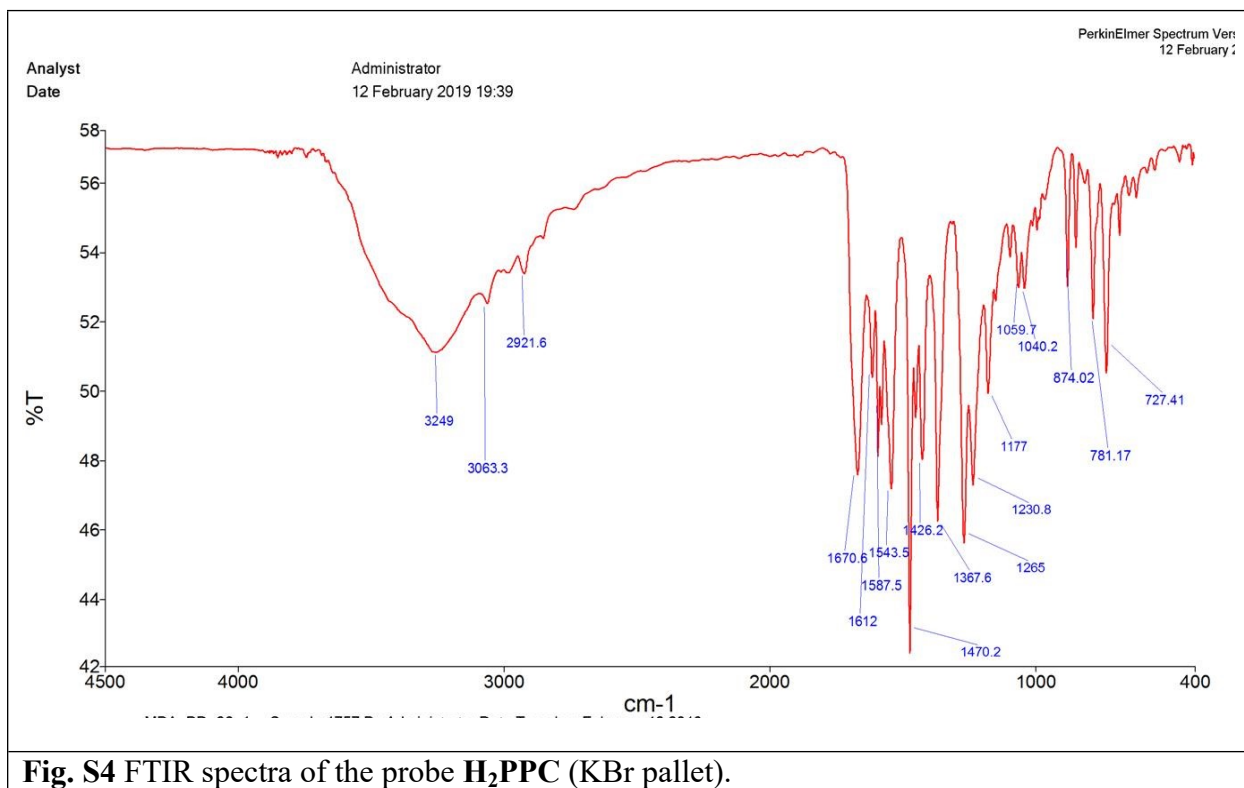
**Fig. S1** :  $^1\text{H}$  NMR of the ligand  $\text{H}_2\text{PPC}$  (Bruker 500 MHz,  $\text{DMSO-d}_6$ )



**Fig. S2** :  $^{13}\text{C}$  NMR of the ligand  $\text{H}_2\text{PPC}$  (Bruker 125 MHz,  $\text{DMSO-d}_6$ )



**Fig. S3** Mass spectra of ligand  $\text{H}_2\text{PPC}$ . 337.1175 (calculated), 338.1247 (observed) correspond to  $(\text{H}_2\text{PPC} + \text{H}^+)$ , and 360.1155 correspond to  $(\text{H}_2\text{PPC} + \text{Na}^+)$



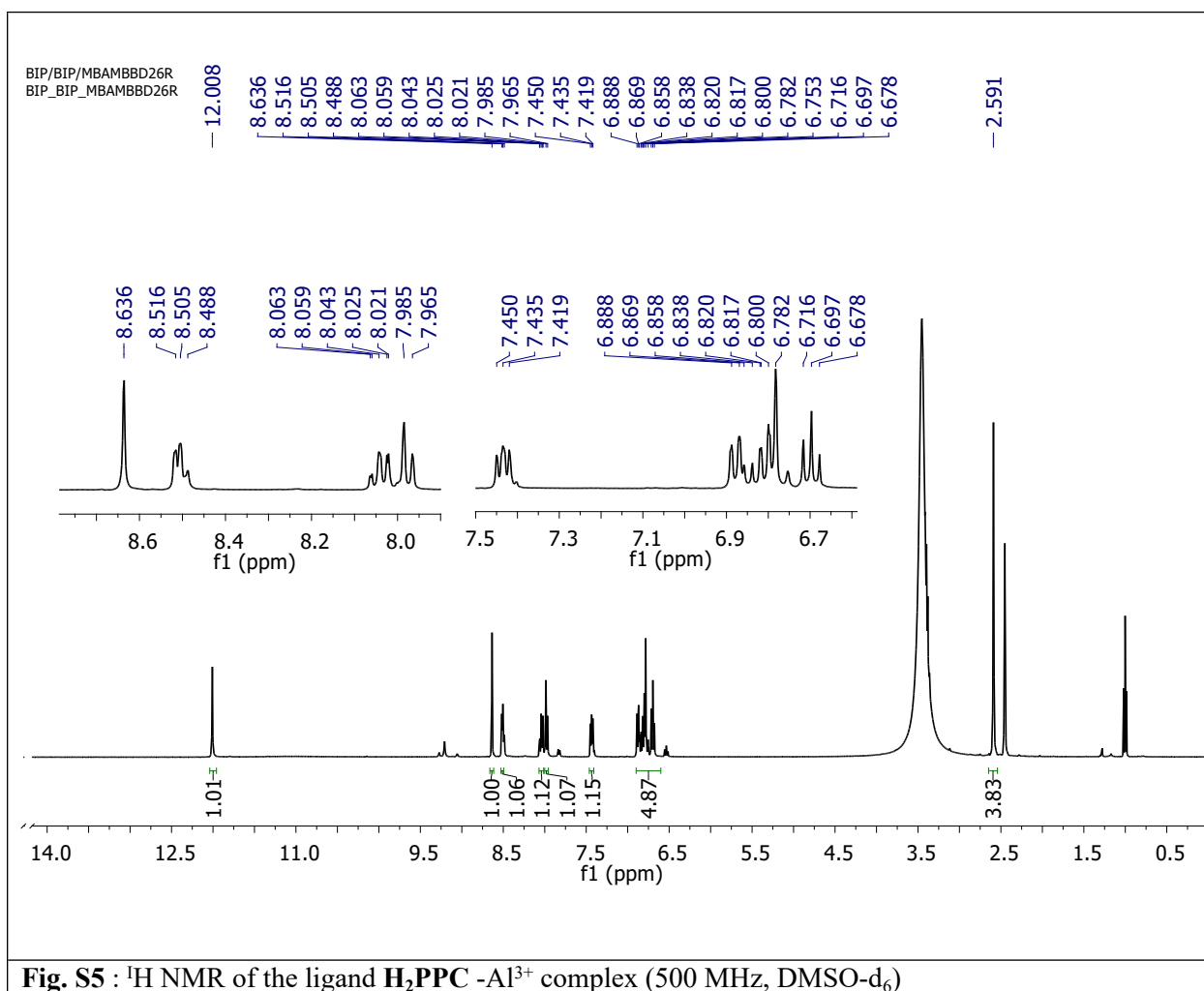
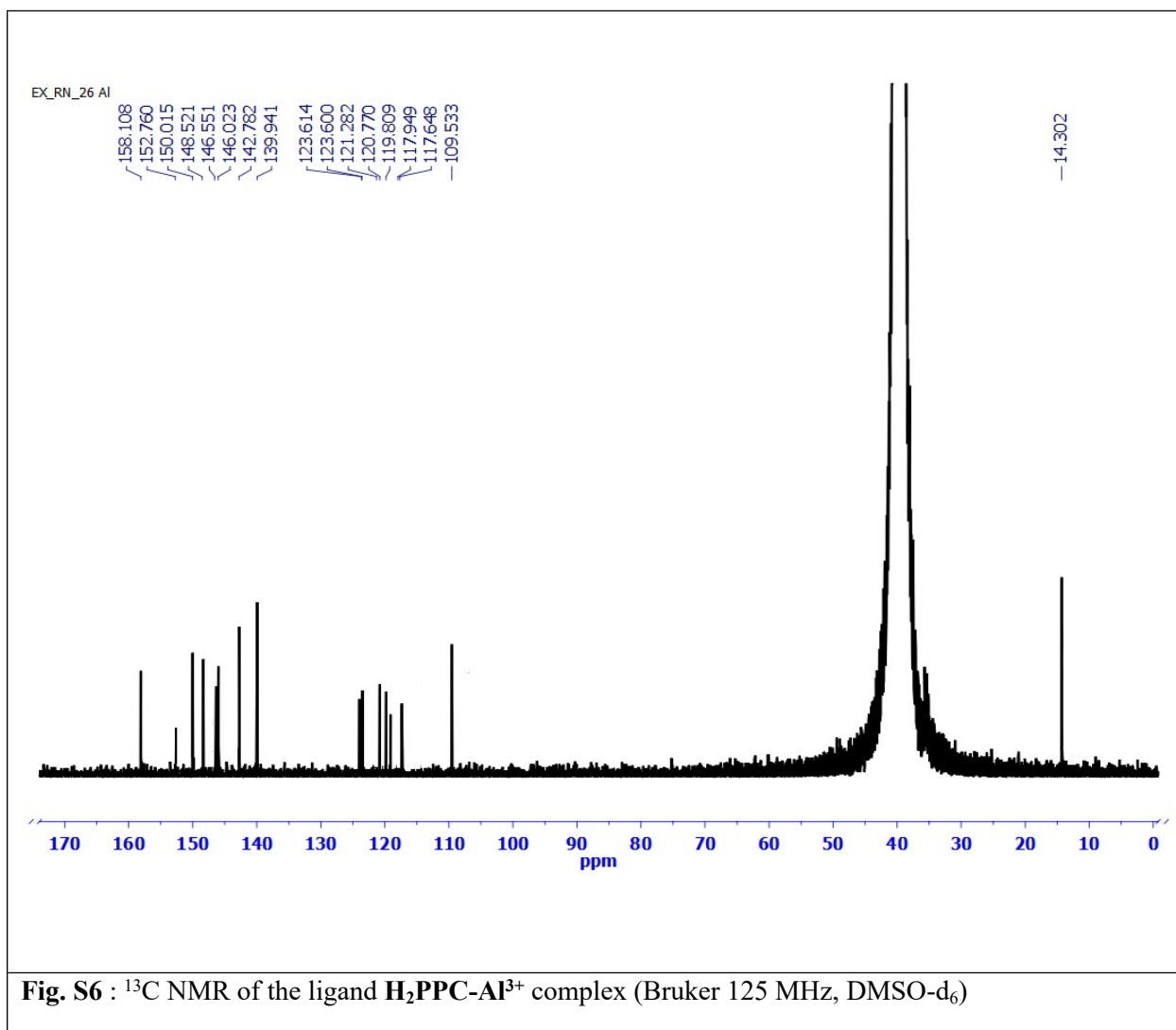


**Fig. S5** :  $^1\text{H}$  NMR of the ligand  $\text{H}_2\text{PPC}$  - $\text{Al}^{3+}$  complex (500 MHz,  $\text{DMSO-d}_6$ )



## Display Report

<b>Analysis Info</b>		Acquisition Date	1/12/2016 12:01:27 PM
Analysis Name	D:\Data\JAN-2016\PM\12012016_PM_TA_SD_MLS.d	Operator	Amit S Sahu
Method	Pso_tune_wide.m	Instrument	micrOTOF-Q II 10337
Sample Name	Bruker micro TOF -Q II		
Comment			

<b>Acquisition Parameter</b>			
Source Type	ESI	Ion Polarity	Positive
Focus	Not active	Set Capillary	4500 V
Scan Begin	50 m/z	Set End Plate Offset	-500 V
Scan End	3000 m/z	Set Collision Cell RF	650.0 Vpp
		Set Nebulizer	0.4 Bar
		Set Dry Heater	180 °C
		Set Dry Gas	4.0 l/min
		Set Divert Valve	Waste

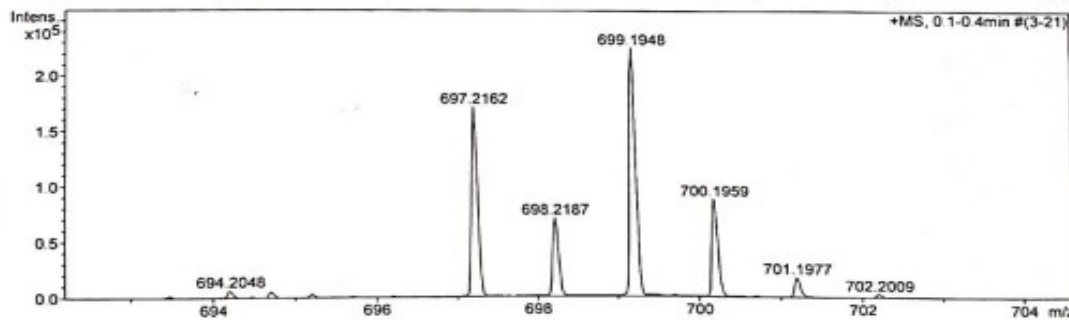
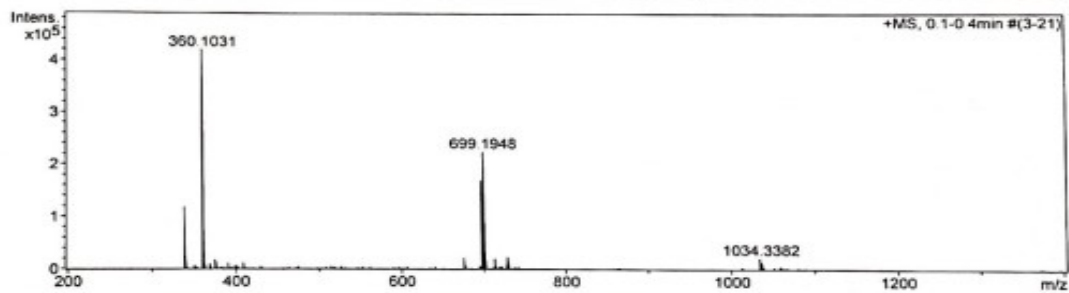
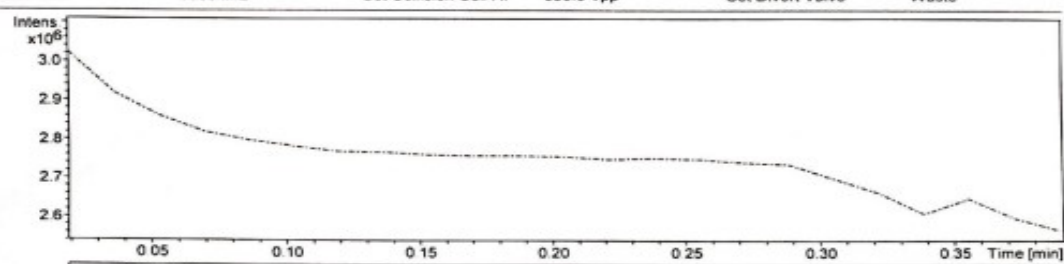


**Fig. S7** Mass spectra of the  $\text{H}_2\text{PPC} + \text{Al}^{3+}$  complex (2:1). Calculated 699.2009, observed 699.1948 correspond to  $[\text{2H}_2\text{PPC} + \text{Al}^{3+} - 2\text{H}^+]$



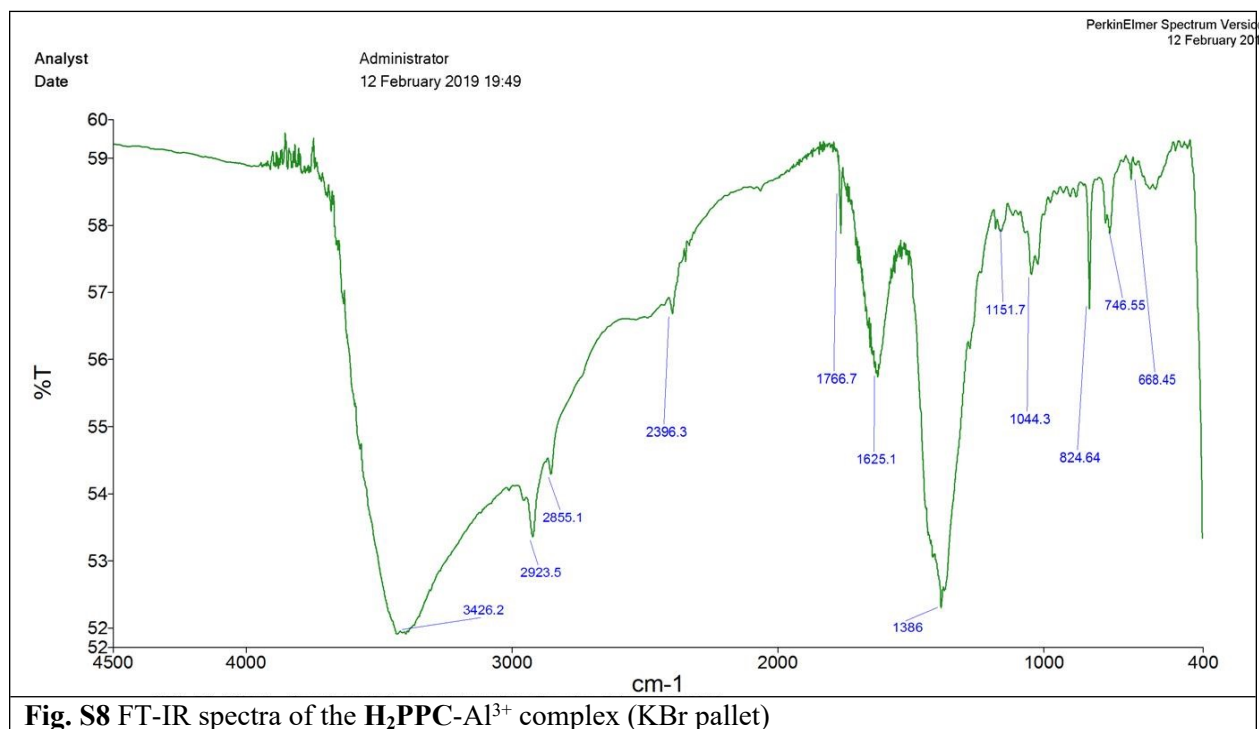


**Fig. S8** FT-IR spectra of the  $H_2PPC-Al^{3+}$  complex (KBr pallet)

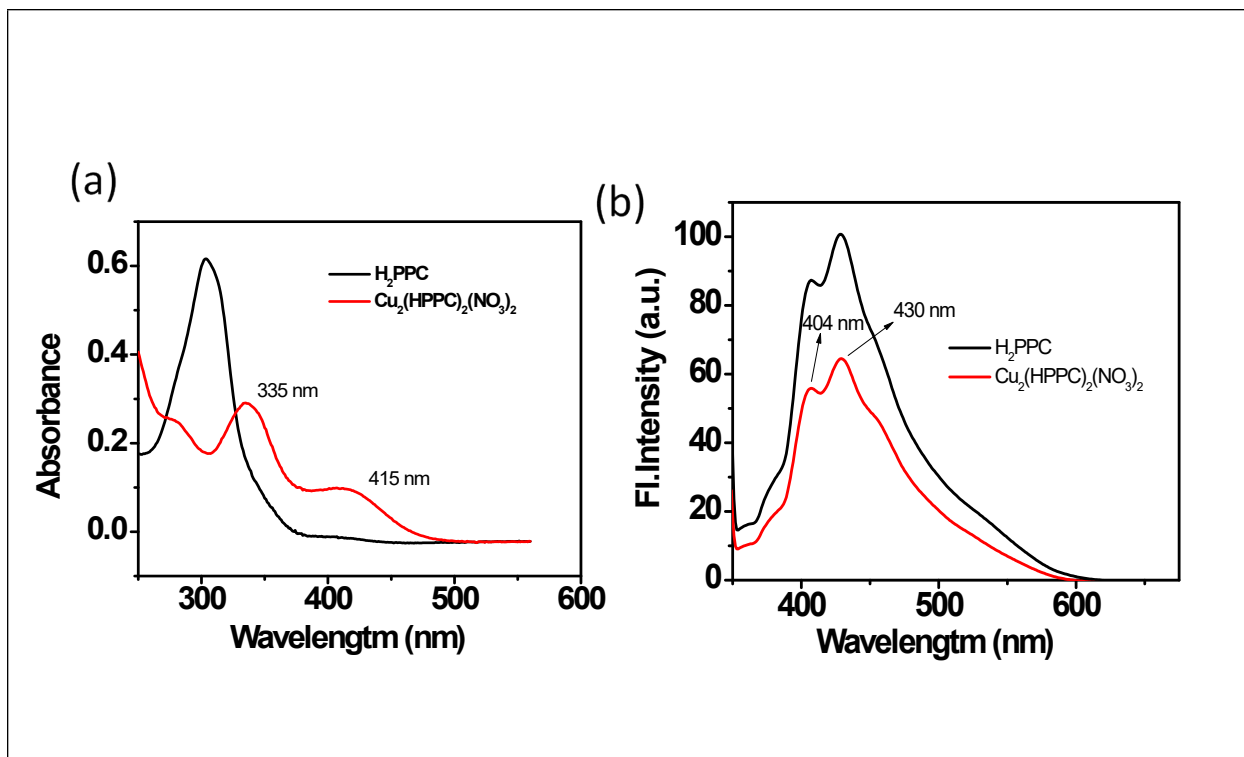


Fig. S9 : (a) absorption spectra and (b) emission spectra ( $\lambda_{ex} = 340 \text{ nm}$ ) of  $H_2PPC$  and  $H_2PPC-Cu^{2+}$  complex in MeOH- $H_2O$  (9:1, v/v)

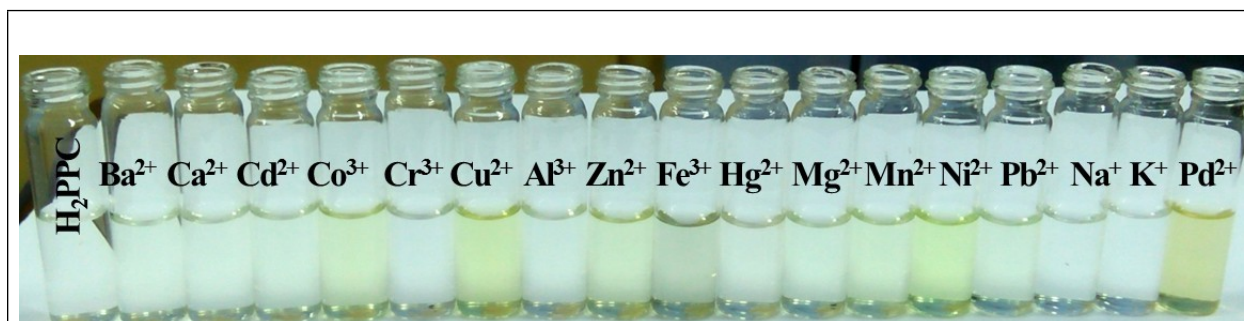
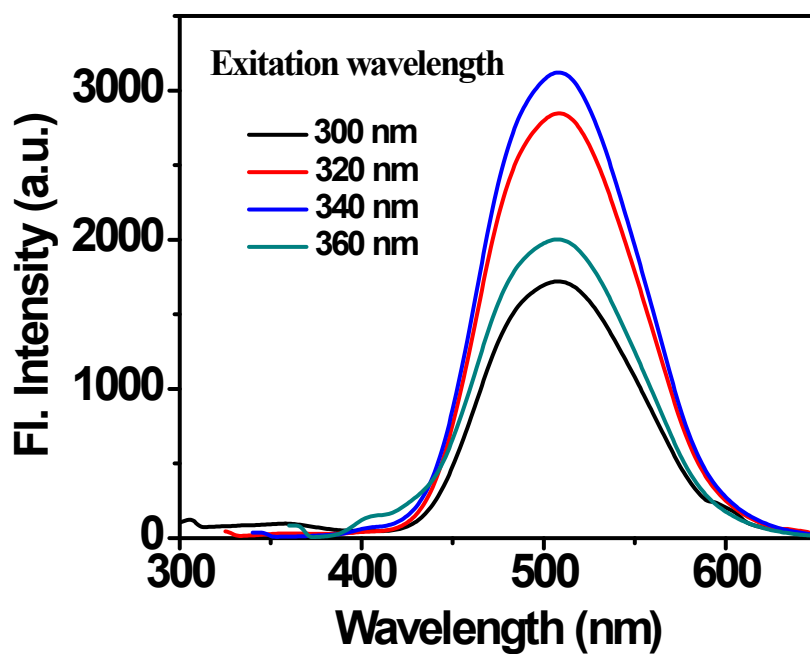


Fig. S10 photographic image of  $H_2PPC$  + different metal ions under ambient light in MeOH- $H_2O$  (9:1, v/v)



**Fig. S11** Graph for excitation wavelength variation of H<sub>2</sub>PPC with Al<sup>3+</sup> in MeOH-H<sub>2</sub>O (9:1, v/v)

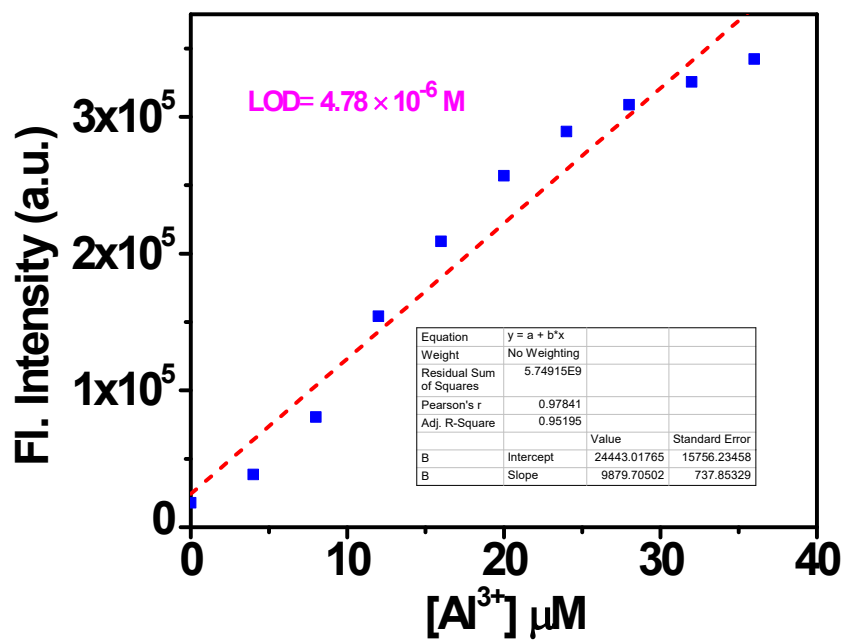
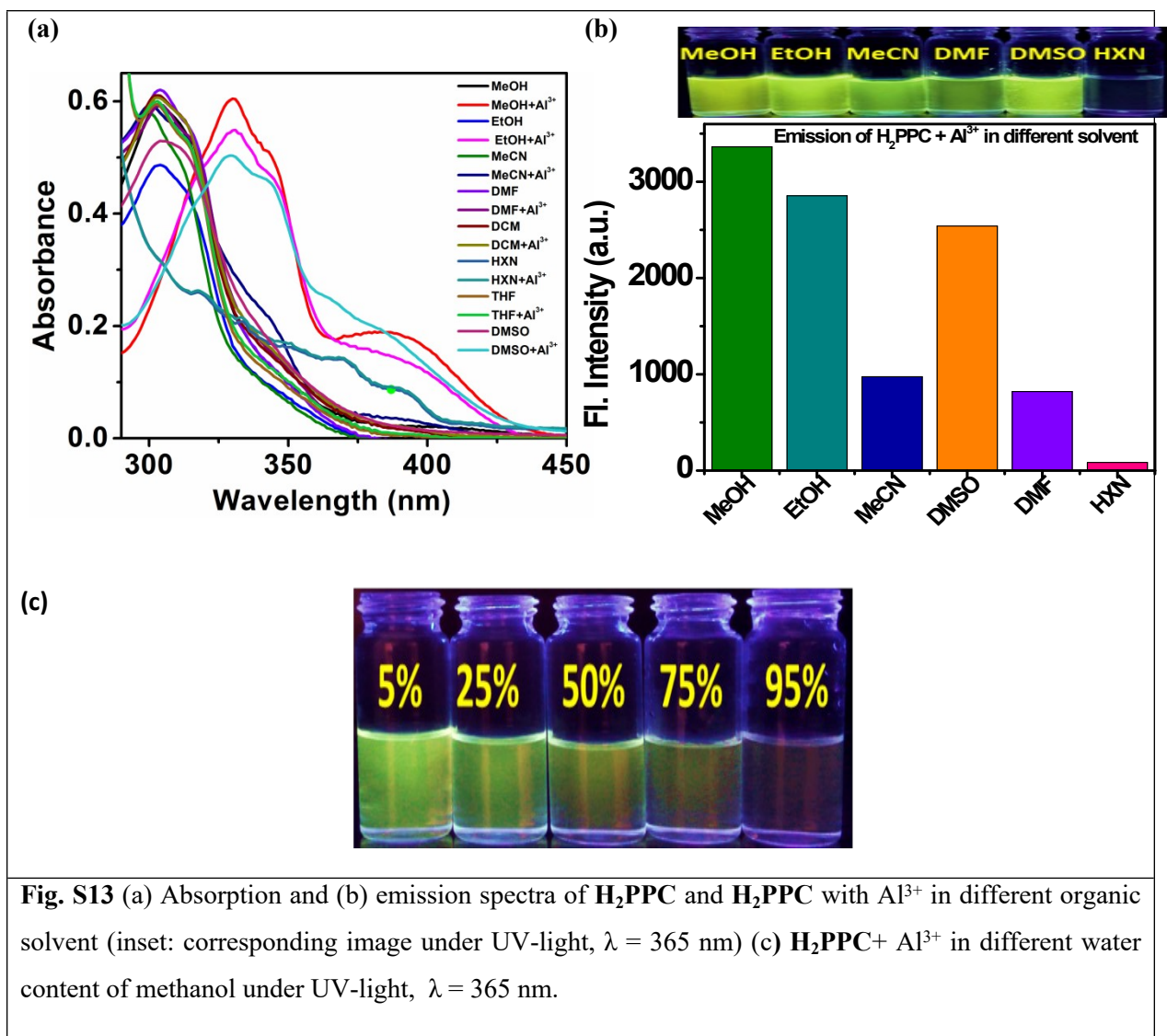


Fig. S12 plot for calculation of detection limit





**Fig. S14** Jobs' plot from fluorescence titration results

**Table-S1**

Crystallographic data of **H<sub>2</sub>PPC** and **2**

Empirical formula	C <sub>17</sub> H <sub>15</sub> N <sub>5</sub> O <sub>3</sub> ( <b>H<sub>2</sub>PPC</b> )	C <sub>34</sub> H <sub>28</sub> Cu <sub>2</sub> N <sub>12</sub> O <sub>12</sub> ( <b>2</b> )
Formula weight	337.34	923.78
Crystal system	Tetragonal	Triclinic
Space group	I41/a (No. 88)	P-1 (No. 2)
a/ Å	19.559(2)	8.4663(13)
b/ Å	19.559(2)	9.2044(14)
c/ Å	16.966(3)	11.8424(18)
α/°	90	73.774(2)
β/°	90	70.534(2)
γ/°	90	80.563(2)
V/Å <sup>3</sup>	6490.4(15)	832.9(2)
Z	16	1
Density(D/gcm <sup>-3</sup> )	1.381	1.842
μ/mm <sup>-1</sup>	0.098	1.368
F(000)	2816	470
Temperature(K)	150	100
Θ range for data collection <sup>0</sup>	1.6, 25.9	1.9, 28.0
Dataset	-23: 19 ; -23: 23 ; -20: 20	-9: 11 ; -11: 11 ; -11: 15
Tot., Uniq. Data, R(int)	14751, 2939, 0.038	9623, 3719, 0.046
Observed data [I > 2.0 σ(I)]	1798	3071
Nref, Npar	2939, 239	3719, 280
R, wR2, S	0.0419, 0.1150, 1.01	0.0578, 0.1653, 1.10

**Table-S2**

Selected bond distances (Å) and angles (°) data for **2**

Selected Bonds	Value(Å)	Selected Angles	(°)
Cu1-O3	1.897(2)	O3-Cu1-O4	91.58(12)
Cu1-O4	2.357(3)	O3-Cu1-N1	98.08(13)
Cu1-N1	2.053(4)	O3-Cu1-N3	172.53(14)
Cu1-N3	1.919(3)	O3-Cu1-N5	95.48(13)
Cu1-N5	2.010(4)	O3-Cu1-O3 <sup>#</sup>	84.69(11)
Cu1-O3 <sup>#</sup>	2.730(3)	O4-Cu1-N1	97.53(13)
		O4-Cu1-N3	95.42(14)
		O4-Cu1-N5	83.01(13)
		O3 <sup>#</sup> -Cu1-O4	171.62(9)
		N1-Cu1-N3	78.45(14)
		N1-Cu1-N5	166.41(13)
		O3 <sup>#</sup> -Cu1-N1	90.43(12)
		N3-Cu1-N5	87.97(15)
		O3 <sup>#</sup> -Cu1-N3	88.70(12)
		O3 <sup>#</sup> -Cu1-N5	89.86(12)

		Cu1-O3-Cu1 <sup>#</sup>	95.31(12)
--	--	-------------------------	-----------

Symmetry  $\# = 1-x, 1-y, -z$

**Table-S3**

Details of hydrogen bond distances (Å) and angles (°) of **H<sub>2</sub>PPC** and complex-**2**

Compound	D-H...A	d(D-H)	d(H...A)	d(D...A)	<(DHA)
<b>H<sub>2</sub>PPC</b>	N4-H4N ...O1	0.87(2)	2.167(19)	2.963(2)	152.6(16)
	O2-H2 ...N5	0.99(3)	1.73(3)	2.600(2)	145(3)
Complex-2	N4-H4N ...O6	0.75(6)	2.32(6)	2.969(6)	145(6)
	O2-H2O ...O5	0.85(6)	2.15(6)	2.774(5)	129(6)

**Table S4:** Ionic radii and ionic potential of relevant cations

Cations	Ionic radius <sup>a</sup> (Å)	Ionic potential (Z/r)	Hydrated radius <sup>b</sup> (Å)	Ionic potential (z/r)
Na <sup>+</sup>	0.95	1.05	3.58	0.279
K <sup>+</sup>	1.33	0.75	3.31	0.302
Ba <sup>2+</sup>	1.35	1.48	4.04	0.495
Ca <sup>2+</sup>	0.99	2.02	4.12	0.485
Cd <sup>2+</sup>	0.97	2.06	4.26	0.469
Co <sup>2+</sup>	0.72	2.63	4.23	0.472
Cr <sup>3+</sup>	0.64	4.68	4.61	0.650
Cu <sup>2+</sup>	0.72	2.78	4.19	0.477
Zn <sup>2+</sup>	0.74	2.70	4.30	0.465
Al <sup>3+</sup>	0.50	6	4.75	0.631
Fe <sup>3+</sup>	0.60	5	4.57	0.656
Hg <sup>2+</sup>	1.02	1.96	-	-
Mg <sup>2+</sup>	0.65	3.07	4.28	0.467
Mn <sup>2+</sup>	0.80	2.50	4.38	0.456
Ni <sup>2+</sup>	0.70	2.85	4.04	0.495
Pb <sup>2+</sup>	1.32	1.51	4.01	0.498



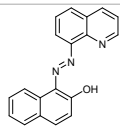
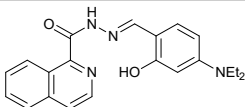
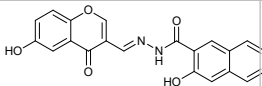
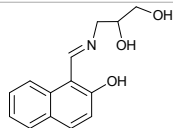
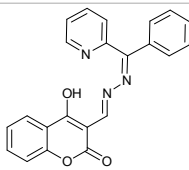
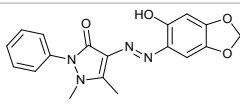
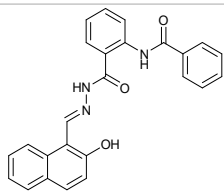
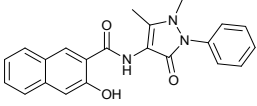
a L. Pauli "Nature of the Chemical Bond," Cornell University Press, 2nd. ed., Ithaca, N. Y., 194,

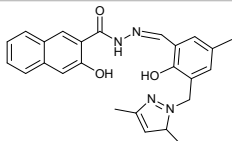
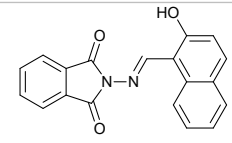
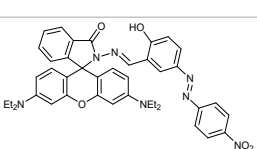
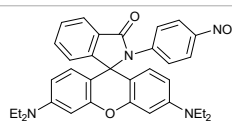
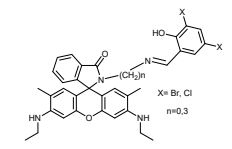
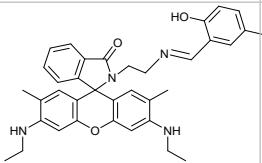
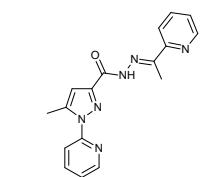
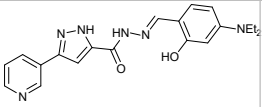
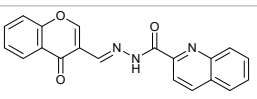
<sup>b</sup> E.R. Nightingale, Phenomenological theory of ion solvation. effective radii of hydrated ions, *J. Phys. Chem. C* 63 (1959) 1381–1387

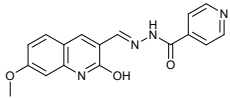
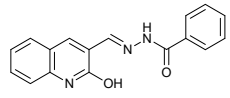
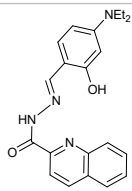
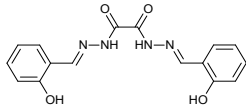
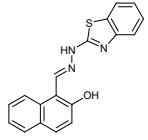
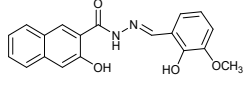
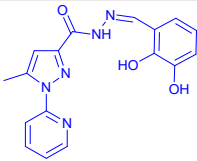
**Table S5:** Selective bond distance and bond angles of **1** from DFT

Bond	Bond distance(Å)	Bond	Bond angles(°)
A11-O1	1.865	N1-A11-O1	87.23
A11-O2	1.890	O1-A11-O2	89.82
A11-N1	1.971	N1-A11-O2	80.92
A11-N2	1.929	N1- A11-N2	105.13
A11-N3	1.999	O1- A11-N2	163.75
A11-N4	1.951	O2- A11-N2	81.95
		N3- A11-N4	103.82
		O1- A11-N3	80.93
		O1- A11-N4	93.53
		O2- A11-N3	87.14
		O2- A11-N4	168.91

**Table S6:** some recent published work on Al<sup>3+</sup> sensor

Sl	Sensor Structure	Excitation and emission maxima (nm)	Medium	Detection limit	Interference	Paper strip based sensing	imaging in Live Cell	Reference
1		537, 612	H <sub>2</sub> O	0.69 Nm	No cations, F-	yes	no	1
2		467, 545	MeOH	0.5 Nm	Cu <sup>2+</sup> , Co <sup>2+</sup> , Ni <sup>2+</sup> , Fe <sup>2+</sup>	no	MCF-7	2
3		435, 503	EtOH:H <sub>2</sub> O (3: 1, v/v)	0.348 Nm	Cu <sup>2+</sup> , Ni <sup>2+</sup> , Fe <sup>3+</sup>	yes	NO	3
4		307, 436	MeOH:H <sub>2</sub> O (2:8, v/v)	45 μM	NO	no	HepG2 cell	4
5		380, 481	MeOH:H <sub>2</sub> O (1:1, v/v)	3.91Nm	Co <sup>2+</sup> , Ni <sup>2+</sup>	yes	AGS cells	5
6		450, 613	MeOH:H <sub>2</sub> O	35 μM	no	yes	no	6
7		430, 480	MeOH:H <sub>2</sub> O (8:2)	1.68 Nm	no	yes	MDA-MB-468	7
8		360, 505	MeOH	28 nm	Fe <sup>3+</sup>	no	no	8

9		487, 493	MeOH-H <sub>2</sub> O (4:6)	114 nM	no	yes	HepG2	9
10		375, 472	DMSO-H <sub>2</sub> O (1:9 v/v)	1 ppb	nd	yes	no	10
11		500, 582	EtOH-H <sub>2</sub> O (4:1)	11 μM	no	NO	NO	11
12		490, 578	MeCN/H <sub>2</sub> O 1:8	0.3 μM	no	yes	zebrafish brain tissue	12
13		345, 555	MeOH-H <sub>2</sub> O (1:9)	1.4-5.3 nM	no	NO	MDA-MB-468	13
14		500, 552	MeOH-H <sub>2</sub> O (9:1)	2.86 nM.	Cu <sup>2+</sup> , Fe <sup>3+</sup> , Ni <sup>2+</sup> and Co <sup>2+</sup>	No	E. coli, B.s ubtilis C. albican E. histolytica	14
15		300, 450	DMSO-H <sub>2</sub> O (2:8)	1.2 nM	no	yes	HepG2	15
16		400, 468	H <sub>2</sub> O, HEPES	0.062 μM	Cu <sup>2+</sup>	no	HeLa cell	16
17		435, 520	MeOH-H <sub>2</sub> O (7:3,v/v)	7.6 nM	F-	no	Verocells	17

18		380, 443	water	56 nM	PPi	no	MCF-7	18
19		390, 442	HEPES buffer	0.72 nM	Cu <sup>2+</sup> and Fe <sup>3+</sup>	Yes	no	19
20		390, 440 and 480 590 ,	MeCN-H <sub>2</sub> O (1:4)	0.104, 4.17 μM	no	no	HeLa cells	20
21		410, 491	bis-tris buffer	2.01 μM	Cu <sup>2+</sup> , Fe <sup>2+</sup> , Fe <sup>3+</sup> , Co <sup>2+</sup> , Ni <sup>2+</sup> and Cr <sup>3+</sup>	no	HeLa cells	21
22		420, 515	DMSO-H <sub>2</sub> O (7:3)	ND	Fe <sup>2+</sup> , Fe <sup>3+</sup> , Cu <sup>2+</sup>	NO	NO	22
23		330, 524	MeOH-HEPES buffer (9:1)	1.7 μM	Cu <sup>2+</sup>	YES	no	23
24	 <b>H<sub>2</sub>PPC</b>	340, 506	MeOH-HEPES buffer (9:1)	4.78 μM	Cu <sup>2+</sup> , Fe <sup>3+</sup> , H <sub>2</sub> PO <sub>4</sub> <sup>-</sup>	yes	Vero cell, A549 cells	This work

### Details of other spectroscopic and related biological measurement and analysis:

Details of general method for UV-Vis and PL studies, Detection limit calculation <sup>24</sup> , Fluorescence quantum yield calculation <sup>24</sup>, Fluorescence lifetime measurements <sup>25-27</sup>, Computational details <sup>28-37</sup>, Cell Culture and Imaging Study <sup>38-40</sup> and Cytotoxicity assay <sup>41</sup> were performed according to literature. The related description incorporated in the supporting information part, Page S20-S23, ESI).

### 2.3 General method for absorbance and emission measurements

The stock solution of chemosensor **H<sub>2</sub>PPC** (1.0 mM) was prepared in methanol. The solution of **H<sub>2</sub>PPC** was then diluted to 20 μM with methanol. Solutions of the guest metal cations (c = 10 mM) were prepared in de-ionized water (15 μM HEPES buffer, pH 7.2) for metal selectivity. For titration experiments, solutions of desired concentration of cations were prepared separately. For investigating the metal ion selectivity of the sensor **H<sub>2</sub>PPC** and in titration experiments, quartz cells of 1 cm optical path length were filled with 2 mL solution of **H<sub>2</sub>PPC** (20 μM) to which stock solutions of the metal ions were gradually added using a micropipette. UV–Vis and fluorescence spectra were recorded after 2 minutes of addition of metal salt. For fluorescence measurements, excitation was provided at 340 nm, and emission was acquired from 360 nm to 650 nm with 5 nm E<sub>x</sub> bandwidth and 5 nm E<sub>m</sub> bandwidth. All the measurements were taken at room temperature.

## 2.4 Limit of Detection (LOD) calculation

The limit of detection for Al<sup>3+</sup> was calculated from the fluorescence titration applying the equation<sup>24</sup>

$$LOD = 3\sigma / \kappa$$

Where  $\sigma$  is the standard deviation of blank measurement, and  $\kappa$  is the slope between the fluorescence emission intensity versus [Al<sup>3+</sup>]. The slope was obtained from the plot of the fluorescence emission intensity at wavelength 506 nm vs. concentration of [Al<sup>3+</sup>].

## 2.5 Fluorescence quantum yield measurements

Fluorescence quantum yields ( $\phi$ ) were determined using the following equation:

$$\Phi_{sample} = \frac{OD_{standard} \times A_{sample}}{OD_{sample} \times A_{standard}} \times \Phi_{standard}$$

Where A represents the area under the fluorescence spectral curve and OD symbolizes the optical density of the compound at the excitation wavelength 340 nm. Fluorescein in 0.1M NaOH ( $\phi = 0.79$ ) was taken as the reference compound to measure the fluorescence quantum yield.

## 2.6 Fluorescence lifetime measurements

Fluorescence lifetimes were measured by Time Correlated Single- Photon Counting (TCSPC) method using a HORIBA Jobin Yvon Fluorocube-01-NL fluorescence lifetime spectrometer. The sample was excited using a laser diode at 375 nm and the signals were collected at the magic angle of 54.7° to eliminate any considerable contribution from fluorescence anisotropy decay<sup>25</sup>. The typical time resolution of our

$$\tau_{av} = \frac{\sum \alpha_i \tau_i^2}{\sum \alpha_i \tau_i}$$

experimental setup is  $\sim 100$  ps. The decays were deconvoluted using DAS-6 decay analysis software. Mean (average) fluorescence lifetimes were calculated using the following equation<sup>26,27</sup>:

in which  $\alpha_i$  is the pre-exponential factor corresponding to the  $i^{\text{th}}$  decay time constant,  $\tau_i$ .

## 2.7 Computational details

Ground state electronic structure calculations in the gas phase of the ligand and complex have been carried out using the DFT<sup>28</sup> method associated with the conductor-like polarizable continuum model (CPCM).<sup>29,30</sup> Becke's hybrid function<sup>31</sup> with the Lee-Yang-Parr (LYP) correlation function<sup>32</sup> was used for the study. The absorbance spectral properties in MeOH medium for **H<sub>2</sub>PPC** and **[Al(HPPC)<sub>2</sub>]<sup>+</sup>(1)**, were calculated by time-dependent density functional theory (TDDFT)<sup>33–35</sup> associated with the conductor-like polarizable continuum model and we computed the lowest 40 singlet – singlet transition.

For H atoms we used 6-31(g) basis set; for C, N, O and Al atoms we employed 6-31+g as basis set for all the calculations. The calculated electron-density plots for frontier molecular orbitals were prepared by using Gauss View 5.1 software. All the calculations were performed with the Gaussian 09W software package.<sup>36</sup> Gauss Sum 2.1 program<sup>37</sup> was used to calculate the molecular orbital contributions from groups or atoms.

## 2.8 Cell Culture and Imaging Study

(ia) Human lung cancer cell lines A549 were purchased from National Centre for Cell Science (NCCS, India) and was well maintained in heat-inactivated FBS (fetal bovine serum, 10%) containing Dulbecco's Modified Eagle's Medium (DMEM) added with 100 mg/mL concentration of antibiotics viz. penicillin, streptomycin, gentamycin and amphotericin B (fungizone). Cells were incubated in a chamber humidified with 5% CO<sub>2</sub> to achieve 70%–80% of confluence prior to the imaging experiment.

### (ib) In vitro live cell imaging of Al<sup>3+</sup> in A549 cells

In vitro imaging of Al<sup>3+</sup> in live cells was executed according to previous methods.<sup>38, 39</sup> For in vitro imaging studies, the cells were seeded in 12-well tissue culture plates with a seeding density of 10<sup>5</sup> cells per well. After reaching 70%–80% confluence, the previous DMEM medium was replaced with serum free DMEM medium. Then **H<sub>2</sub>PPC** (10  $\mu$ M) was incubated for 2 hours to facilitate cellular uptake. After then the cells were washed three times with PBS to remove any free ligand present. After then, the cells were incubated further with Al<sup>3+</sup> (50  $\mu$ M) for 45 minutes in fresh serum-free DMEM. Images of live cells were then taken by using an EVOS® FL Cell Imaging System, Life Technologies, USA.

### (ii) Cell Culture of Vero Cells

Vero Cells were cultured in Dulbecco's Modified Eagle Medium (DMEM) with 5–10% fetal bovine serum (FBS). A monolayer of cells ( $1.0 \times 10^6$  cells/ml) was grown onto 6-well plates in a humidified incubator at 5% CO<sub>2</sub> for 24 h at 37 °C. The cells were fixed in paraformaldehyde (4%) solution and blocked with 1% bovine serum albumin (BSA) in 0.1% PBS (phosphate-buffered saline)-Triton-X100 solution and were washed and then permeabilized with 0.1% Triton-X100 in PBS.

### (ii) In vitro fixed cell imaging of Al<sup>3+</sup> in Vero cell

The permeabilized Vero cell monolayer was treated with the ligand **H<sub>2</sub>PPC** (50 μM) for 30 min and washed twice with PBS (pH 7.2) to eliminate cell debris.<sup>39,40</sup> The cells were subsequently incubated with an aqueous solution of Al<sup>3+</sup> as Al(NO<sub>3</sub>)<sub>3</sub> (100 μM) for 30 min, washed twice with PBS, and were observed under an epifluorescence microscope.

### (iii) Cytotoxicity assay:

In vitro cytotoxicity was measured by using the colorimetric methyl thiazolyltetrazolium (MTT, Sigma-Aldrich, Germany) assay against A549 cells according to the previous report.<sup>39,41</sup> The Cells were seeded into 24-well tissue culture plate in presence of 500 μL Dulbecco's modified eagle medium (DMEM) supplemented with 10% fetal bovine serum (FBS) and 1% penicillin/streptomycin at 37°C temperature and 5 % CO<sub>2</sub> atmosphere for overnight and then incubated for 6-12 hours in presence of **H<sub>2</sub>PPC** at different concentrations (10-100 μM). Then cells were washed with PBS buffer and 500 μL supplemented colorless DMEM medium was added. Subsequently, 50 μL of 3-(4,5-dimethylthiazol-2-yl)-2,5-diphenyltetrazolium bromide MTT (5 mg/mL) was added to each well and incubated for 4 hours. Next, violet formazan was dissolved in 500 μL of sodium dodecyl sulfate solution in water/DMF mixture. In order to measure the viable number of cells, the absorbance of solution was measured at 570 nm using microplate reader. The numbers of viable cells were determined by analyzing the percent live cells against untreated controls. The individual values for three replicate determinations were calculated and their mean values are reported.

## References

- 1 C. Sen, S. Dey, C. Patra, D. Mallick and C. Sinha, *Anal. Methods*, 2019, **11**, 4440–4449.
- 2 Y. Wang, Z.-Y. Ma, D.-L. Zhang, J.-L. Deng, X. Chen, C.-Z. Xie, X. Qiao, Q.-Z. Li and J.-Y. Xu, *Spectrochim. Acta Part A Mol. Biomol. Spectrosc.*, 2018, **195**, 157–164.
- 3 B. jie Pang, C. rui Li and Z. yin Yang, *J. Photochem. Photobiol. A Chem.*, 2018, **356**, 159–165.

- 4 B. Naskar, D. K. Maiti, A. Bauzá, A. Frontera, C. Prodhán, K. Chaudhuri and S. Goswami, *ChemistrySelect*, 2017, **2**, 5414–5420.
- 5 S. Gharami, K. Aich, P. Ghosh, L. Patra, N. Murmu and T. K. Mondal, *J. Photochem. Photobiol. A Chem.*, 2020, **390**, 112294.
- 6 G. Bartwal, K. Aggarwal and J. M. Khurana, *New J. Chem.*, 2018, **42**, 2224–2231.
- 7 A. Bhattacharyya, S. C. Makhál and N. Guchhait, *ACS Omega*, 2018, **3**, 11838–11846.
- 8 A. Sen Gupta, K. Paul and V. Luxami, *Anal. Methods*, 2018, **10**, 983–990.
- 9 H. Mohammad, A. S. M. Islam, C. Prodhán, K. Chaudhuri and M. Ali, *Photochem. Photobiol. Sci.*, 2018, **17**, 200–212.
- 10 C.-L. Li, P.-H. Lu, S.-F. Fu and A.-T. Wu, *Sensors*, 2019, **19**.
- 11 S. Mabhai, M. Dolai, S. Dey, A. Dhara, B. Das and A. Jana, *New J. Chem.*, 2018, **42**, 10191–10201.
- 12 S. Das, U. Mukherjee, S. Pal, S. Maitra and P. Sahoo, *Org. Biomol. Chem.*, 2019, **17**, 5230–5233.
- 13 J. Mandal, P. Ghorai, K. Pal, T. Bhaumik, P. Karmakar and A. Saha, *ACS Omega*, 2020, **5**, 145–157.
- 14 A. Roy, R. Mukherjee, B. Dam, S. Dam and P. Roy, *New J. Chem.*, 2018, **42**, 8415–8425.
- 15 B. Naskar, K. Das, R. R. Mondal, D. K. Maiti, A. Requena, J. P. Cerón-Carrasco, C. Prodhán, K. Chaudhuri and S. Goswami, *New J. Chem.*, 2018, **42**, 2933–2941.
- 16 Y. Wang, Y.-F. Song, L. Zhang, G.-G. Dai, R.-F. Kang, W.-N. Wu, Z.-H. Xu, Y.-C. Fan and L.-Y. Bian, *Talanta*, 2019, **203**, 178–185.
- 17 R. Purkait, C. Patra, A. Das Mahapatra, D. Chattopadhyay and C. Sinha, *Sensors Actuators, B Chem.*, 2018, **257**, 545–552.
- 18 S. K. Asthana, A. Kumar, Neeraj, Shweta, S. K. Hira, P. P. Manna and K. K. Upadhyay, *Inorg. Chem.*, 2017, **56**, 3315–3323.
- 19 L. Tian, J. Xue and Z. Yang, *Tetrahedron Lett.*, 2018, **59**, 4110–4115.
- 20 R. Singh, S. Samanta, P. Mullick, A. Ramesh and G. Das, *Anal. Chim. Acta*, 2018, **1025**, 172–180.
- 21 T. G. Jo, J. J. Lee, E. Nam, K. H. Bok, M. H. Lim and C. Kim, *New J. Chem.*, 2016, **40**, 8918–8927.
- 22 N. Xiao, L. Xie, X. Zhi and C.-J. Fang, *Inorg. Chem. Commun.*, 2018, **89**, 13–17.
- 23 U. Saha, B. Das, M. Dolai, R. J. Butcher and G. Suresh Kumar, *ACS Omega*, 2020, **5**, 18411–18423.
- 24 B. Das, A. Jana, A. Das Mahapatra, D. Chattopadhyay, A. Dhara, S. Mabhai and S. Dey, *Spectrochim. Acta - Part A Mol. Biomol. Spectrosc.*, 2019, **212**, 222–231.
- 25 J. R. Lakowicz, *Principles of Fluorescence Spectroscopy*, Plenum, New York, 1999.



- 26 S. Banthia and A. Samanta, *J. Phys. Chem. B*, 2006, **110**, 6437–40.
- 27 B. Ramachandram and A. Samanta, *J. Phys. Chem. A*, 1998, **102**, 10579–10587.
- 28 R. G. Parr, *Horizons Quantum Chem.*, 1980, 5–15.
- 29 V. Barone and M. Cossi, *J. Phys. Chem. A*, 2001, **102**, 1995–2001.
- 30 M. Cossi, N. Rega, G. Scalmani and V. Barone, *J. Comput. Chem*, 2003, **24**, 669–681.
- 31 A. D. Becke, *J. Chem. Phys.*, 1993, **98**, 5648–5652.
- 32 C. Lee, W. Yang and R. G. Parr, *Phys. Rev. B*, 1988, **37**, 785–789.
- 33 R. E. Stratmann, G. E. Scuseria and M. J. Frisch, *J. Chem. Phys.*, 1998, **109**, 8218–8224.
- 34 R. Bauernschmitt and R. Ahlrichs, *Chem. Phys. Lett.*, 1996, **256**, 454–464.
- 35 M. E. Casida, C. Jamorski, K. C. Casida and D. R. Salahub, *J. Chem. Phys.*, 1998, **108**, 4439–4449.
- 36 M. J. Frisch, G. W. Trucks, H. B. Schlegel, G. E. Scuseria, M. A. Robb, J. R. Cheeseman, G. Scalmani, V. Barone, B. Mennucci, G. A. Petersson, H. Nakatsuji, M. Caricato, X. Li, H. P. Hratchian, A. F. Izmaylov, J. Bloino, G. Zheng, J. L. Sonnenberg, M. Hada, M. Ehara, K. Toyota, R. Fukuda, J. Hasegawa, M. Ishida, T. Nakajima, Y. Honda, O. Kitao, H. Nakai, T. Vreven, J. A. Montgomery Jr., J. E. Peralta, F. Ogliaro, M. Bearpark, J. J. Heyd, E. Brothers, K. N. Kudin, V. N. Staroverov, R. Kobayashi, J. Normand, K. Raghavachari, A. Rendell, J. C. Burant, S. S. Iyengar, J. Tomasi, M. Cossi, N. Rega, J. M. Millam, M. Klene, J. E. Knox, J. B. Cross, V. Bakken, C. Adamo, J. Jaramillo, R. Gomperts, R. E. Stratmann, O. Yazyev, A. J. Austin, R. Cammi, C. Pomelli, J. W. Ochterski, R. L. Martin, K. Morokuma, V. G. Zakrzewski, G. A. Voth, P. Salvador, J. J. Dannenberg, S. Dapprich, A. D. Daniels, Ö. Farkas, J. B. Foresman, J. V. Ortiz, J. Cioslowski and D. J. Fox, *Gaussian Inc.*, 2009, Wallingford CT.
- 37 A. L. Tenderholt, K. M. Langner and N. M. O’Boyle, *J. Comput. Chem.*, 2008, **29**, 839–845.
- 38 S. Guria, A. Ghosh, K. Manna, A. Pal, A. Adhikary and S. Adhikari, *Dye. Pigment.*, 2019, **168**, 111–122.
- 39 P. Bag, D. Chattopadhyay, H. Mukherjee, D. Ojha, N. Mandal, M. C. Sarkar, T. Chatterjee, G. Das and S. Chakraborti, 2012, 1–12.
- 40 R. Purkait, C. Patra, A. Das and D. Chattopadhyay, *Sensors Actuators B. Chem.*, 2017, **257**, 545–552.
- 41 S. Guria, A. Ghosh, P. Upadhyay, M. K. Das, T. Mishra, A. Adhikary and S. Adhikari, *ACS Appl. Bio Mater.*, 2020, **3**, 3099–3113.

\*\*\*\*\*